Modeling of Retinal Electrical Stimulation Using a Micro Electrode Array Coupled with the Gouy-Chapman Electrical Double Layer Model to Investigate Stimulation Efficiency

F.Dupont[*,1], R.Scapolan[1], J-F.Bêche[1], C.Condemine[1] , M.Belleville[1], P.Pham[1]
[1]CEA, LETI, Minatec, Grenoble, France
*Corresponding author: 17 rue des martyrs 38054 Grenoble Cedex, florent.dupont@cea.fr

Abstract: Electrical stimulation for retinal implant has known significant improvements in the last decades with many implantations and experimentations. The ability to create better controlled and better adapted stimulation signals to increase efficiency is a major objective. In this paper, we present a model describing cell excitability to electrical stimuli and its numerical framework, based on COMSOL Multiphysics 3.5a. The mathematical model is based on the AC Electrokinetic Complex Equation coupled to the Gouy-Chapman model of the Electrical Double Layer (EDL). The EDL is formed at the interface between the electrode surface and the extracellular medium. In order to validate those mathematical models, we compared numerical simulations of retinal nine-element Platinum Micro Electrode Array (MEA) with impedance spectroscopy measurements for sinusoidal low amplitude stimuli. Thanks to the positive outcome of the comparison, we were able to start the evaluation of different and more complex stimuli waveforms using in particular the Fast Fourier Transform algorithm (FFT). The retinal MEA used during the measurement campaign was manufactured at CEA.

Keywords: Electrical Simulation, Retinal Ganglion Cell, Electrical Double Layer, Finite Element Method, COMSOL

1 Introduction

Blindness issues due to Retinis Pigmentosa (RP) and Age Related Macular Degeneration (AMD) are diseases affecting the retina and leading to loss of vision. Cures of different types (drugs, surgery, etc.) are being investigated and several attempts at using electrical stimulation have already been made [1]. Most of the studied cases have seen about 30% of the Retinal Ganglion Cells (RGC) remain functional even years after RP or AMD screening.

Retinal prostheses are generally made of an extraocular part recording visual images and of an intraocular part providing electrical stimuli to excitable RGC. The inner device generally consists in an integrated circuit delivering electrical signals to an MEA.

Besides damage associated to mechanical shocks, many studies have shown that electrical stimulation patterns can lead to permanent damage caused by irreversible electrochemical reactions. Thus, biphasic charge-balanced waveforms are preferred to monophasic waveforms when stimulation is applied to single electrodes. Damage caused by electrical stimulation is related to the stimulation pulse's amplitude and frequency, but more important, to the charge density and the charge per phase [2].

Those findings have a direct impact on the electrode design and on the electrical waveform used for the stimulation. Likewise, from an electrical point of view, efficiency of a stimulation system is also related to the design of the electrodes (pattern and individual dimensions) and the shape of the applied waveforms. Optimization of any electrode-waveform system can be conducted through modeling incorporating elements describing the biological response.

Some geometry aspects have already been investigated with numerical simulation of different brain electrode types using FEM modeling [3]. This study deals with the design dimensions for 2D/3D electrodes to make stimulations more efficient and safer. Cantrell & al [4] defined different stimulation waveforms based on well known shapes such as Gaussian and sinus. They compared their efficiencies with the empirical square waveform mostly used by clinicians. Theses comparisons are made in order to show an improvement on the amount of charges needed to elicit tissue responses without damaging tissue.

Other approaches consisting in an improvement of efficiency by taking into account the spatio-temporal aspect of stimuli are also being investigated: Valente & al. [5] explained that some phased arrays stimuli could

modify the tissue response behavior. This modeling study is only applied to Deep Brain Stimulation (DBS). Those improvements are leading to new ways in designing stimulators and prosthetic devices.

The previously mentioned studies [3-5] are examples showing many ways of studying the electrical stimulation in living tissues and yet presenting modeling as the starting point. Our objective is to propose a numerical framework which will allow us to optimize our electrodes geometries and the electrical waveform in order to design more efficient and safe retinal prosthesis. In this paper, we present the mathematical models chosen for representing the living matter and the impedance measurements done to assert the validity of those choices.

2 Ruling equations: Hodgkin-Huxley and AC Complex Electrokinetic

The model has to represent four contributions:
(i) the applied stimulus, (ii) the EDL formed at the electrode surface, (iii) the bulk part of the extracellular medium and the RGC seen as real dielectrics, (iv) the RGC specific electrical activity.

Applied stimuli are non sinusoidal. We use the FFT approach and decompose this temporal signal into a sum of sinusoids (see section 3).

2.1 Modeling of cells and extracellular medium bulk

RGC and the bulk part of the extracellular medium are real dielectrics of conductivity σ and permittivity ε. For sinusoidal stimuli and under the linear assumption, the electrical potential distribution is described by the electrokinetic complex equation [6]:

$$\vec{\nabla}.\left(-\sigma^{*}\vec{\nabla}V_{0}^{*}\right)=0 \qquad (1)$$

Where σ^{*} is the complex conductivity and V_0^* the magnitude of the complex electrical potential. Associated boundaries conditions (BCs) are of Neumann homogeneous type to represent insulated boundaries:

$$-\sigma^{*}\vec{\nabla}V_{0}^{*}.\vec{n}=0 \qquad (2)$$

$\vec{n}$ is the outer normal vector at insulated boundary. MEA contacts polarization induces a capacitive behavior of the electrode-electrolyte interface. Counter-ions of the electrolyte are attracted to the charged electrode and create a capacitive Electrical Double Layer (EDL). Considered as a thin layer approximation due to its very small width (Debye length λ_d is about 8nm for the extracellular medium), the EDL is modeled with the following Robin boundary condition [6]:

$$-\sigma^{*}\vec{\nabla}V_{0}^{*}.\vec{n}=-i\omega C_{GC}\Delta V \qquad (3)$$

Where ΔV is the potential drop across the EDL and C_{GC} the Gouy-Chapman EDL capacitance:

$$C_{GC}=\frac{\varepsilon_{eau}}{\lambda_d} \qquad (4)$$

For the particular case of a saline solution without the presence of retinal tissues (*in vitro* condition), equation (1) coupled to BC (3) should behave like an electrical RC series circuit.

In this study, we first use the GC EDL linear model to represent the EDL capacitance. Many more realistic non linear models for the EDL are available in literature: the replacement of C_{GC} in BC (3) is possible if needed [7].

2.2 Modeling of RGC electrical activity

Neural information transfer in the inner retina is performed by Action Potentials (AP), also referred to as spikes. An AP is a short-lasting event in which the electrical trans-membrane potential rapidly rises and falls, following a stereotyped waveform. APs occur in several types of animal excitable cells including RGCs (neuron type).

Electrical stimulation of excitable cells either increases the AP firing rate (increase of activity) or inhibits it. Hodgkin–Huxley (HH) equations describe how APs in neurons are initiated and propagated. This set of nonlinear Ordinary Differential Equations (ODE) approximates the electrical characteristics of neurons [8]. A diffusion term was added to take account for the AP propagation along the axon:

$$\frac{a}{2\rho_i}\frac{\partial^2 V_m}{\partial x^2}=C_m\frac{dV_m}{dt}+\bar{g}_{Na}m^3h(V_m-E_{Na})+\bar{g}_K n^4(V_m-E_K)+\bar{g}_L(V_m-E_L) \qquad (5)$$

$$\frac{dm}{dt} = \alpha_m(1-m) - \beta_m m \quad (6)$$

$$\frac{dh}{dt} = \alpha_h(1-h) - \beta_h h \quad (7)$$

$$\frac{dn}{dt} = \alpha_n(1-n) - \beta_n n \quad (8)$$

Where Im, Vm and Cm are respectively trans-membrane current, voltage and capacitance. α_k and β_k are opening and closing time constants of membrane ionic channels and $\overline{g}_k$ are conductivities associated to those channels. As a first step, RGC activity can be modeled by those HH equations even if some authors proposed more refined models [8].

3 The Fast Fourier Transform for non sinusoidal stimuli

To be able to use the complex formalism of the electrokinetic equation (1), only sinusoidal signals can be used as stimuli. However, most of the empirical stimuli used are periodic but non sinusoidal. A possible way to accommodate this limitation is to decompose a discrete temporal signal into a finite sum of sinusoids with discrete frequencies.

The computationally efficient FFT is a widely used algorithm to calculate Discrete Fourier Transform (DFT). In order to benefit from the FFT efficiency, the number of samples (N) must be a power of two. This transform is the link between the discrete temporal and the discrete frequency signals representation. The whole FFT algorithm is largely and exhaustively explained in the original text [9].

Any T periodic signal x(t) with a completely arbitrary shape can be sampled respecting the Shannon theorem $T_{sampling} \geq T/2$ to give:

$$x[n] = x(nT_{sampling}), n \in [0, N-1] \quad (9)$$

If $N \not\equiv 0(2)$, it is possible to add zeros at the end of the sampled signal x[n] to complete the sequence without altering the results [9].

$$X[m] = FFT[x] = \sum_{n=0}^{N-1} x[n] e^{-\frac{2\pi j n m}{N}} \quad (10)$$

The Fourier coefficients X[m] are complex values that contain both phase and amplitude information of the sinusoid of frequency $mF_{sampling}/N$. The module versus frequency plot is displayed in figure 1 for various signal waveforms. Those selected waveforms are typical stimulation elementary patterns.

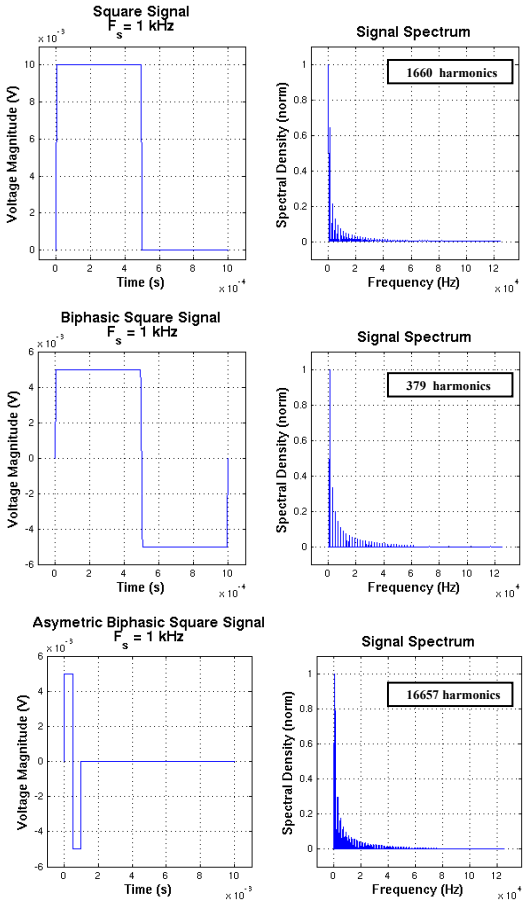

Figure 1. Different types of FFT input waveforms with a display of the spectral information obtained after algorithm processing (One-sided spectrum)

This figure emphasizes the fact that a different waveform means a different spectral content. Thus the number of harmonics is varying from 379 (biphasic square signal) to 16657 (asymmetric biphasic square signal).

The FFT is a reversible transform allowing recreation of x[n] from X[m] through the FFT^{-1} transform:

$$x[n] = FFT^{-1}[X] = \frac{1}{N}\sum_{m=0}^{N-1} X[m] e^{-\frac{2\pi j n m}{N}} \quad (11)$$

Finally, there are two essential points of interest in the use of the FFT algorithm for us:

(i) The decomposition in sinusoidal elements is notably matching with the underlying hypothesis when using the complex electrokinetic equation. In fact, those sinusoidal elements are eigen functions of the linear filter represented by GC Capacitance and the bulk resistance which means that the output will preserve inputs sinusoidal characteristics.

(ii) The enabled reverse transform leads to the possibility to decompose and recompose every arbitrary temporal waveform.

4 Use of COMSOL Multiphysics

4.1 COMSOL Multiphysics interface

The AC Electrokinetic Complex Equation (1) coupled to the GC capacitance EDL model was implemented in the Partial Differencial Equations (PDE) module. The equation is solved using a stationary direct linear solver and the solution is extracted as an M-file. The language description of the FEM solution allows the parameter sweep such as the signal frequency and amplitude. The insertion of those varying parameters in a COMSOL script brings flexibility to simulations and post-processing.

4.2 MATLAB

It is therefore possible to implement the following method starting with the M-file extracted COMSOL script in order to provide its inputs and to process its outputs. The entire script is written and ran as a MATLAB file:

- Creation of the signal
- N-points FFT of the signal (equation 10)
- Loop on positive frequencies (N/2+1)
  - Solve in COMSOL
  - Saving of strategic values
- Switch one-sided to two-sided spectrum
- N_points iFFT of the signal (equation 11)
- Post-processing

Multiple fields can be asserted in the script such as geometry dimensions, boundaries mesh or post processing values. The recording of several points of the current and voltage waveform can be performed using the ‘postint’, ‘posteval’ and 'postcrossplot’ functions.

Finally, the switch to two-sided spectrum and the FFT^{-1} function use (‘ifft’) lead to temporal signals reconstruction and display.

5 Validation of numerical simulations with impedance spectroscopy

The numerical model was solved for a Micro Electrode Array (MEA) made of nine Platinum contacts (Ø=40µm), nine counter electrodes (CE, width=10µm) and a general counter electrode (GCE, width=20µm). This MEA was developed and manufactured at CEA.

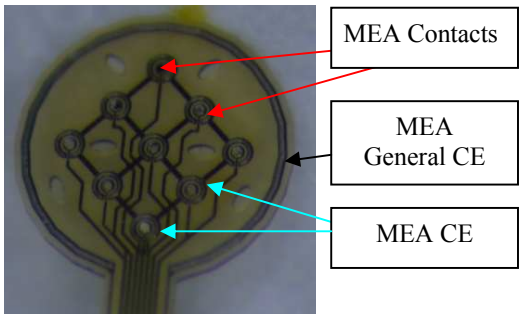

Figure 2. Picture of the MEA-RETINE showing the nine platinum circular contacts and the counter-electrodes.

Impedance measurements were first done using the GCE as the working electrode. A millimetric Platinum circular electrode, immersed in the electrolyte, was used as the CE. The test setup used for the impedance measurements was composed of a VMP-2 potentiostat (Bio-logic company [10]), electronic switch array to select both the MEA contacts and the CEs. The MEA bathes into a Phosphate Buffered Solution (PBS) solution. The PBS is a water-based solution containing several types of ions such as sodium, potassium and chloride. The osmolarity and the ion concentrations of PBS usually match those of the human body. The conductivity of PBS was measured at 1.6 S/m at room temperature (25°C).

The potentiostat was used in Potentio Electrochemical Impedance Spectroscopy (PEIS) mode. This mode executes a frequency sweep at the desired threshold and displays the impedance response. The working electrode (WE) can be either a contact, or a CE, or the GCE or any electrode present in the electrolyte.

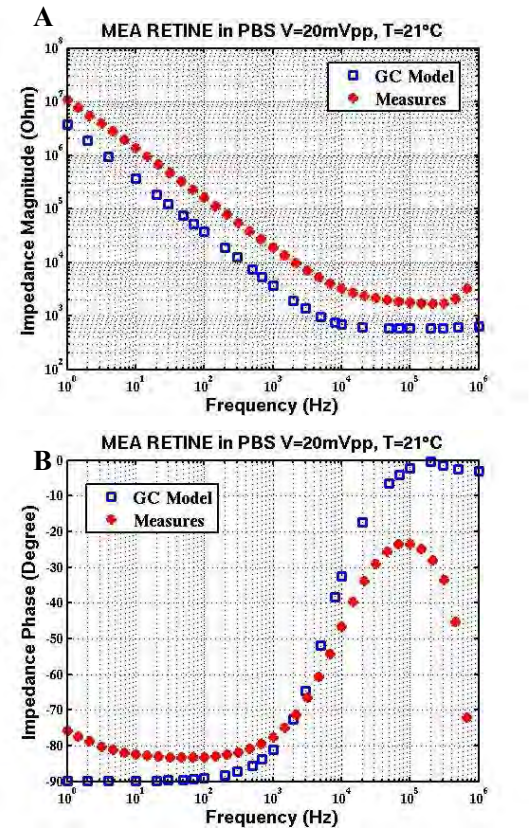

Figure 3. Impedance Bode plots for 20mV peak to peak (red), comparison to numerical results (blue). The GCE is used as the working electrode and the CE is a circular millimetric electrode immersed in PBS. A/ impedance module. B/ impedance phase.

As already said, the electrode-electrolyte system is assimilated to a RC series circuit. The R resistance corresponds to the high-frequency plateau. The module plot (A) shows that measured bulk resistance is underestimated by numerical simulations. At low frequency, the main effect is due to the capacitance though there is still a mismatch between measurements ad calculations. This might come from the WE geometry which is not identical between simulations and the actual one. Indeed a post study shows that the etching of all contacts and CE was non complete. As a result, the resistance seen at the interface was underestimated and the capacitance surface was diminished.

Additionally, the GC model assumed the EDL capacitance to be constant and its use inside a complex formulation showed that it is just a first-order approximation [6].

Finally, it must be said that the potensiostat VMP-2 upper frequency limit is 1 MHz so we assume that the phase drop is mostly due to the setup limits (unreliable above 0.5MHz).

6 Limitations of the framework

6.1 Spectrum Magnitude Threshold

When the one-sided spectrum is selected in the script, it is possible to determine a threshold which will reject the low amplitude peaks from the solving loop. As noted on figure 1 the waveform shape is directly influencing the number of spectrum harmonics and in turn the loop iterations number. The objective is to optimize the computation time without degrading the signal quality.

In figure 4, plots A and B show how the signal response quality decreases with the threshold increase. Accuracy validation is the key to properly interpret the future results of our experimental patterns. With the A plot, we estimate that a threshold over 10^{-5} AU (Arbitrary Units) will contain too many oscillations to give proper results. With the B plot, for a threshold over 10^{-6} AU, the curve becomes too polluted by unbalanced sinusoids.

The harmonics amount given on figure 1 was calculated for a null threshold. With threshold of 10^{-5} AU for both case A and B, the spectral content is reduced from 379 to 36 harmonics for biphasic square signal, from 1660 to 96 for monophasic square signal and from 16657 to 793 harmonics for non symmetric square signal. The number of computations is respectively reduced of 91%, 94% and 95%.

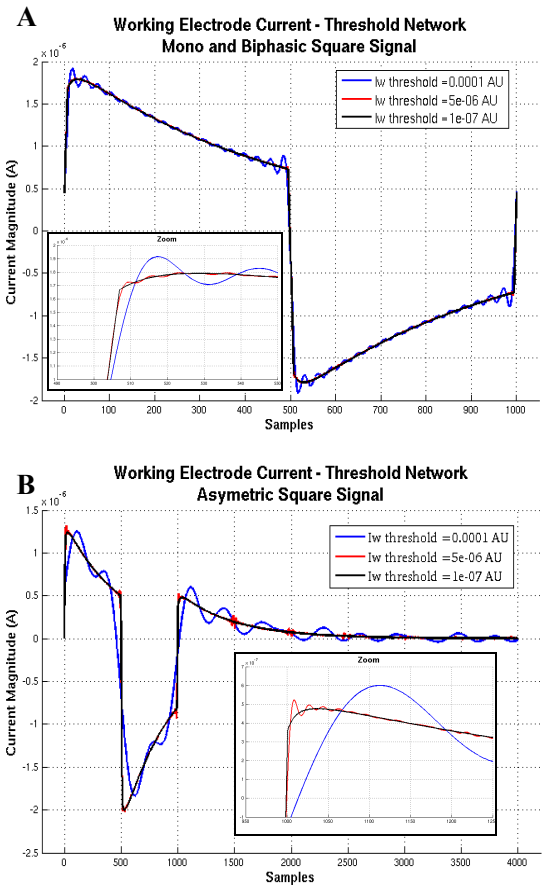

Figure 4. Current waveform spectra according to threshold values. A/ Observation of the waveform shape for mono and biphasic square signal B/ Observation of the waveform shape for asymmetric biphasic square signal.

6.2 Working and Counter Electrode Mesh

In the M-File, iterations can be conducted on the boundary maximal element size to modify the mesh resolution. Total current conservation provides information about the mesh quality. The objective is to find an acceptable mesh threshold to reduce the computation time. The central contact and the GCE are respectively used as WE and CE for this calculation simulation.

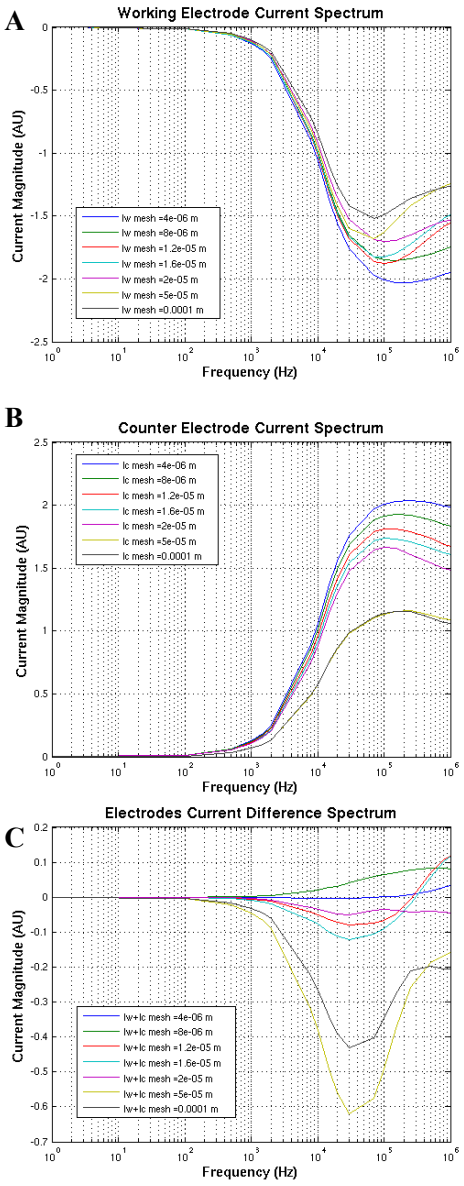

Figure 5. Current spectra according to mesh size. A/ Observation of the crossing current at the WE (negative current) B/ Observation at the CE (positive current) C/ Difference to appreciate the right mesh.

We can verify the high pass filter behavior of the electrode-electrolyte system. In both A and B, the current begins to significantly cross the electrode-electrolyte interface around 100Hz. A small unexpected drop is observed above 200kHz, which can be attributed to the numeric model. As displayed in figure 5, the finer the mesh is, the higher the current is (A and B) and

the smaller the error is (C). The 10-µm mesh value (maximum element size) seems to be the best compromise providing both high accuracy and reasonable computation time.

7 Retinal Ganglion Cell Model

Data was collected at key geometry points to be evaluated during the post-processing phase. Thus the temporal voltage signal was used as a real stimulus and its capability to initiate an AP will be evaluated. A classic Heaviside step function was chosen to evaluate the implementation of this temporal model.

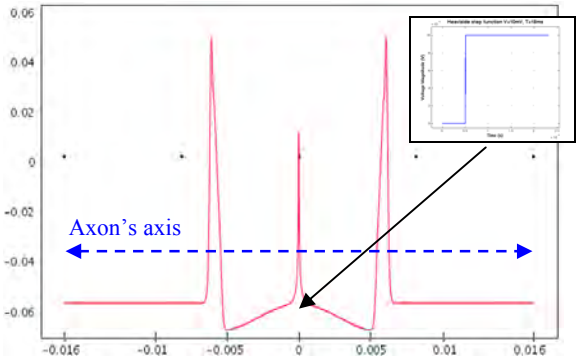

Figure 6. Trans-membrane AP response to a 10-mV Heaviside step function stimulus in the middle of the axon, 10ms after stimulation.

Figure 6 shows that the 1-µm-radius axon's response to a Heaviside step function stimulus applied in the middle of the axon. As expected, this artificial stimulation leads to the creation of two identical APs propagating in opposite directions at $1.1 m.s^{-1}$.

8 Conclusion

In order to obtain a numerical framework to investigate the response of the electrode-electrolyte-cell system to arbitrary electrical stimulation waveforms, two models were implemented (electrokinetic complex and HH equations). The FFT algorithm was used to decompose the complex-variable stimulation patterns in frequency-magnitude vectors. The model's simulation results were compared with impedance measurements. The manufacturing process of the RETINE-MEA is still maturing and some problems were pointed out by the discrepancies between our model and the measurements. Computation time optimization can be achieved by setting thresholds on the signal spectral density (number of harmonics to be considered) and on the mesh resolution. After verifying the accuracy of our procedure with simple rectangular waveforms, the framework is now ready to accept arbitrary signal waveforms in order to investigate stimulation safety and efficiency.

Acknowledgment

The authors would like to thank Mr Sadok Gharbi, Mr Stéphane Bonnet and Mr Laurent Gerfault from the CEA-LETI for helpful discussions and suggestions and Mr Fabien Sauter for the lending of the MEA-RETINE.

References

1. W. Mokwa, "Artificial retinas",Comprehensive Microsystems, Oxford: ElsevierScience Eds. Gianchandani, Tabata, 201–217 Vol.3, 2007.
2. D. B. McCreery , W. F. Agnew, T. G. H. Yuen , et al. "Charge density and charge per phase as cofactors in neural injury induced by electrical stimulation", *IEEE Trans Biomed Eng*, 996-1001(37), 1990.
3. M. O. Heuschkel, M. Fejtl, M. Raggenbass, D. Bertrand, P. Renaud, "A three dimensional multi-electrode array for multi-site stimulation and recording in acute brain slices", *Journal of Neuroscience Methods*, 135-148, 2002.
4. D. R. Cantrell, J. D. Troy, "Extracellular Stimulation of Mouse Retinal Ganglion Cells with Non-Rectangular Voltage-Controlled Waveforms", *Annual International IEEE EMBS Conference 2009.*
5. V. Valente, A. Demosthenous, R. Bayford, "Application of Phased Array Systems to Deep Brain Stimulation", *IEEE International Conference Electronics Circuits and Systems 2009*
6. P. Pham, R. Scapolan, C. Rubeck and F. Dupont, "Search for a Suitable Numerical Model for Electrical Stimulation: From the Electric Double Layer to Electrokinetics, Confrontation with Impedance Measurements", submitted proceedings of the European Comsol Conference, Paris France, 2010.
7. M. S. Kilic & al, "Steric effects in the dynamics of electrolytes at large applied voltages. I. Double-layer charging", *Physical Review E*, **75**, 2007
8. J. Malmivuo, R. Plonsey, "Bioelectromagnetism", Ed. Oxford University Press, 1995
9. J. W. Cooley, J. W. Tukey, "An Algorithm for The MachineComputation of Fourier Series, Mathematics of Computation", p 297-301, 1965.
10. Bio-logic company, http://www.bio-logic.info/